JCTC Journal of Chemical Theory and Computation

Article

pubs.acs.org/JCTC

Complexes with a Single Metal−Metal Bond as a Sensitive Probe of Quality of Exchange-Correlation Functionals

Serge I. Gorelsky*

Centre for Catalysis Research and Innovation and the Department of Chemistry, University of Ottawa, Ottawa, Ontario K1N 6N5, Canada

Supporting Information

ABSTRACT: The electronic structure of the vanadium dimer complex $[V(C_5H_5)]_2Pn$ with a single metal−metal bond was characterized, and the energies of higher spin states were evaluated. To simplify evaluation of orbital contributions to bonding between atoms and fragments, occupancy-perturbed bond orders were introduced. The structure and experimentally determined singlet−triplet gap in this complex can be used to test the quality of modern exchange-correlation functionals. Most generalized gradient approximation (GGA) functionals were determined to be quite suitable to reproduce the metal−metal distance and the single−triplet energy gap in $[V(C_5H_5)]_2Pn$. Further accuracy improvement can be achieved by using empirical dispersion corrections. Hybrid exchange-correlation functionals, including the B3LYP functional, performed poorly for both structural and energy predictions. The hybrid functionals significantly overestimate the stability of the singlet state with the antiferromagnetically coupled high-spin metal ions relative to the lowest-energy triplet state and the singlet state with stronger metal−metal interactions. Thus, these XC functionals are not quite suitable for computational studies of multinuclear 3d transition metal complexes with weak-to-intermediate metal−metal bonding.

INTRODUCTION

Metal−metal bonding[1−4] is a feature of many transition metal (TM) complexes, especially if metal ions have the d^3, d^4, and d^5 electronic configurations. Two typical 3d TM elements with the propensity to form metal−metal bonds are vanadium and chromium. Recent successes in the synthesis of chromium complexes with very short metal−metal bonds[5−14] resulted in the upsurge of efforts to model the chemical bonding in these complexes using available computational quantum-mechanical methods.[6,9,10,12,13,15−19] However, due to the complex electronic structure of multinuclear complexes with the direct metal−metal interactions,[20] such systems present a significant challenge to modeling.[21,22] For dimer complexes with the singlet ground state, the description of the ground state wave function can range from the closed-shell (CS) singlet with the maximum possible bond order between the metal ions (three for V^{II}−V^{II} complexes, four for Cr^{II}−Cr^{II} complexes, and five for Cr^{I}−Cr^{I} complexes) at very short metal−metal distances to an open-shell (OS) singlet with two antiferromagnetically coupled metal ions with little or no covalent bonding between the metal ions[23,24] at long metal−metal distances (Figure 1).

In 2003, a dinuclear vanadium(II) complex of a dianionic pentalene (Pn^{2-}) ligand was synthesized, and its structure and magnetic properties were characterized.[25] The complex (Figure 2) with a direct metal−metal interaction has a spin-singlet ground state with a fairly short V^{II}−V^{II} interatomic distance (2.54 Å). Temperature-dependent measurements of ^1H NMR spectra have allowed accurate determination of the energy of the low-lying triplet excited state of $[V(C_5H_5)]_2Pn$ ($\Delta H_{singlet-triplet}$ of 4.1 kcal mol^{-1} in toluene). A similar value of $\Delta H_{singlet-triplet}$ (5.7 kcal mol^{-1}) was previously obtained for another V^{II} dimer, $[V(C_5H_5)]_2COT$ (COT = cyclooctatetraene), in toluene.[26] Density functional theory (DFT)

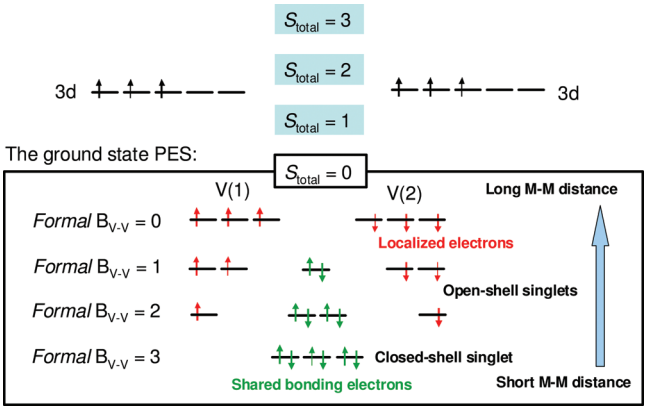

Figure 1. Multiple electronic configurations that originate from the electronic interaction of two V^{II} ions.

calculations at the PBE[27]/TZVP[28] level of theory have established that the singlet ground state of $[V(C_5H_5)]_2Pn$ is an OS singlet with a single metal−metal bond and two unpaired electrons on each V^{II} ion (Figures 1 and 2).[29] The calculated properties for the lowest energy singlet and triplet states (d_{V-V} of 2.57 Å and $\Delta E_{singlet-triplet}$ of 5.3 kcal mol^{-1}) were in agreement with the experimental results. The CS singlet with the stronger metal−metal interaction is an excited state with a shorter metal−metal distance (2.38 Å). Its electronic energy is 12.3 kcal mol^{-1} higher than the electronic energy of the BS singlet.

The presence of low-lying excited states that are accessible via Boltzmann population at ambient temperatures is a

Received: January 8, 2012
Published: February 16, 2012

   dx.doi.org/10.1021/ct3000124 | J. Chem. Theory Comput. 2012, 8, 908−914

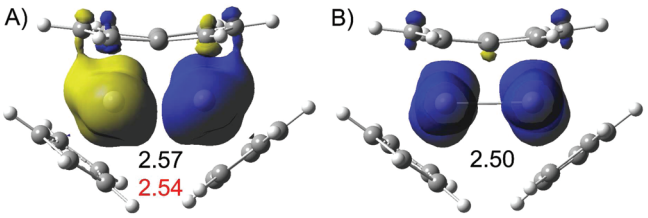

Figure 2. Structure and spin density distribution of (A) the broken-symmetry (BS)[30,31] solution to the open-shell singlet ground state and (B) the lowest-energy triplet excited state of the $[V(C_5H_5)]_2Pn$ complex from PBE/TZVP calculations.[29] The calculated and experimental metal−metal atomic distances (Å) are shown in black and red, respectively. Spin density isosurface value is 0.003.

signature of complexes in which metal−metal interactions are of weak-to-intermediate strengths (the term *partial paramagnetism of a metal−metal bond* has been used in the literature).[32] This feature is absent for systems with very strong metal−metal bonding, such as recently synthesized Cr^{I} and Cr^{II} binuclear complexes, due to the fact that strong metal−metal bonding interactions will push excited states of higher multiplicities to higher energies. As a result, an assessment of quality of a given DFT model for complexes with metal−metal bonds is only based on the comparison of experimental and calculated structural parameters (bond lengths and angles).[33]

Accurate evaluation of energies of high-spin (HS) and low-spin (LS) states of mononuclear TM complexes and spin-coupling parameters for weakly interacting multinuclear TM complexes has been a long-standing issue in modern DFT.[34−39] Ordinary training sets for density functional fits do not contain TM compounds and, thus, do not always represent a balanced data set of chemical compounds.[40] Different exchange correlation (XC) functionals yield results which differ by up to 1 eV for energy order for LS/HS states of 3d TM complexes. A large overstabilization of HS states has been observed for many hybrid functionals. This failure of density functionals was attributed to the fact that HS states are systematically favored in Hartree−Fock-type methods (including DFT with hybrid XC functionals), because Fermi correlation is included in the exact exchange, while Coulomb correlation is not.[34] Petrie and Stranger performed test calculations for 16 charged and neutral binuclear transition-metal complexes.[33] Comparison of experimental and calculated metal−metal distances in these systems using several local density approximation (LDA) and generalized gradient approximation (GGA) functionals indicated that the calculations using gradient-corrected approaches are more accurate for neutral complexes, and structures obtained using the LDA functionals are "overbound" (resulting in too short metal−metal distances). As of now, no comprehensive assessment of the performance of hybrid XC functionals has been undertaken for complexes with metal−metal bonding.

The availability of the X-ray structure and the accurately measured energy of low-lying triplet excited state for $[V(C_5H_5)]_2Pn$ makes this complex very attractive as a testing ground for different levels of DFT. In this paper, the performance of commonly used XC functionals in regard to both geometry and excited state energy predictions is evaluated in order to identify suitable solutions for modeling multinuclear TM complexes with direct metal−metal interactions and to point out levels of theory that should be avoided in computational studies of such systems.

METHODS

All calculations were performed using the Gaussian 09 package.[41] Stationary points on the potential energy surface were obtained using the different XC functionals (PW91,[42,43] BP86,[44,45] PBE,[27] TPSS,[46] VSXC,[47] BLYP,[45,48] G96LYP,[48−50] B97D,[51] PKZB,[52] M06L,[53] TPSSh,[46] τ-HCTH,[54] τ-HCTHhyb,[54] wB97XD,[55] M06,[56] B3P86,[44,57] PBE0,[58,59] BMK,[60] B3LYP,[48,57] X3LYP,[48] and O3LYP[48,61]) and the high-quality, triple-ζ TZVP basis set[28] for all atoms. Tight SCF convergence criteria were used for all calculations. The spin-unrestricted formalism was used for all open-shell calculations. The converged wave functions were tested[62] to confirm that they corresponded to the ground-state surface. The second-order derivatives of the energy with respect to nuclear positions were evaluated to determine the nature of the stationary points. Vibrational zero point energies (ZPE) and thermal corrections were included in the calculation of enthalpies and free energies at 298 K and 1 atm. Empirical dispersion corrections for DFT energies were calculated using the method proposed by Grimme[51] and implemented in the AOMix program.[63−66] DFT calculations with the empirical dispersion corrections are designated accordingly (PBE-D, B3LYP-D, etc.).

The broken-symmetry (BS)[30,31] method was used in calculations for open-shell singlet states. In this method, α- and β-spin electrons occupy two different sets of orbitals. The use of the broken-symmetry solution can be understood as attempting to circumvent the static correlation error of the XC functional.[67] Generation of the initial guess wave functions from the converged fragment wave functions (one fragment is the Pn^{2-} ligand (the closed shell); the other two fragments are the $[V(C_5H_5)]^{+}$ ions with $S = 3/2$ each; these spins are antiferromagnetically coupled to give the dimer with $S_{total} = 0$) for the BS calculations were carried out using the AOMix program.

Since BS wave functions usually suffer from a spin contamination of higher spin states, Yamaguchi's approximate spin-projection method[68,69] can be employed to obtain the energy of the *pure* singlet state. The Heisenberg exchange coupling constant J from the energies of the HS and BS states (E_{HS} and E_{BS}, respectively) is calculated by

$$J = -\frac{E_{HS} - E_{BS}}{\langle \hat{S}^2 \rangle_{HS} - \langle \hat{S}^2 \rangle_{BS}} \quad (1)$$

Here, the expectation values of the spin-squared operator for the HS and BS determinants appear in the denominator. The energy of the pure singlet state E_{OS} is then given by

$$E_{HS} - E_{OS} = -J \times S_{HS}(S_{HS} + 1) \quad (2)$$

In calculations for the pure singlet state of $[V(C_5H_5)]_2Pn$, the HS state is the septet ($S_{HS} = 3$).

Calculation of two-center Mayer bond orders (B_{A-B})[70] between atoms and larger molecular fragments:

$$B_{A-B} = \sum_{a \in A} \sum_{b \in B} [(\mathbf{PS})_{ab}(\mathbf{PS})_{ba} + (\mathbf{P}^{s}\mathbf{S})_{ab}(\mathbf{P}^{s}\mathbf{S})_{ba}] \quad (3)$$

and the analysis of molecular orbitals (MOs) in terms of atomic and fragment orbital (FO) contributions[63,65,71] were carried out using the AOMix program.

dx.doi.org/10.1021/ct3000124 | J. Chem. Theory Comput. 2012, 8, 908−914

To evaluate contributions of individual occupied MOs to bonding between different atoms, orbital occupancy-perturbed (OOP) Mayer bond orders are introduced (eq 4):

$$B^{*}_{A-B} = \sum_{a\in A}\sum_{b\in B}[(\mathbf{P}_X\mathbf{S})_{ab}(\mathbf{P}_X\mathbf{S})_{ba} + (\mathbf{P}^{s}_X\mathbf{S})_{ab}(\mathbf{P}^{s}_X\mathbf{S})_{ba}] \quad (4)$$

New total and spin density matrix elements ($\mathbf{P}_X$ and $\mathbf{P}^{s}_X$, respectively) are calculated for the system with the original set of MOs, but one electron is taken out from a given molecular orbital (Scheme 1), and then these "orbital occupancy perturbed" (OOP) density matrices are used to calculate OOP bond orders (B_{A-B}*).

Scheme 1. Reference Electronic State and Corresponding Occupancy Perturbed States in Which an Electron Is Removed from One Occupied Molecular Orbital (HOMO, HOMO−1, HOMO−2, etc.) or Added to an Unoccupied Molecular Orbital (LUMO, LUMO+1, etc.)[a]

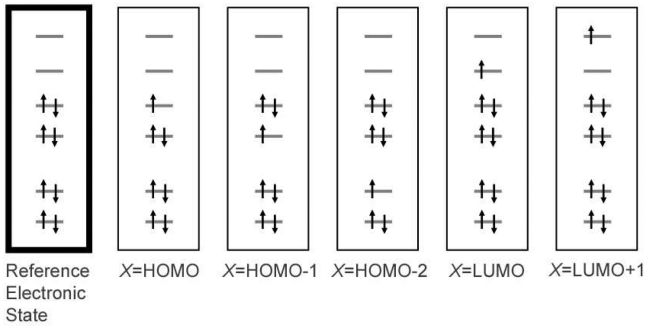

[a]A closed shell reference state is used for simplicity.

OOP bond orders can also be used to evaluate the effects of electron population of unoccupied molecular orbitals. Automatic calculation of OOP bond orders has been implemented in the AOMix software (see Table S1 in the Supporting Information). Usage of OOP bond orders for the analysis of the electronic structure of $[V(C_5H_5)]_2Pn$ will be demonstrated below.

RESULTS AND DISCUSSION

There are two main features in the description of the electronic structure of $[V(C_5H_5)]_2Pn$. The first is the metal−metal bonding while the second arises from the metal−Pn ligand interactions. For the metal−metal bonding, the important interplay is between the spin localization and the bond formation (Figure 1).[20] In order to reproduce structure and the singlet−triplet energy gap in the complex, the metal−metal and metal−ligand interactions should by handled by the XC functional in a balanced way, similar to how these functionals have to treat anisotropic metal−ligand covalency.[72,73]

By using the spin-unrestricted PBE calculations, the electronic energies (with and without the empirical dispersion correction) and metal−metal bond orders were calculated as functions of the metal−metal distance (Figure 3) for (a) the BS singlet with the unpaired electrons on each V^{II} center antiferromagnetically coupled to those of the other metal center, (b) the CS singlet with all electrons paired, and (c) the higher spin states (triplet S = 1, pentet S = 2, and septet S = 3). The calculated potential energy surfaces (PESs) show that the

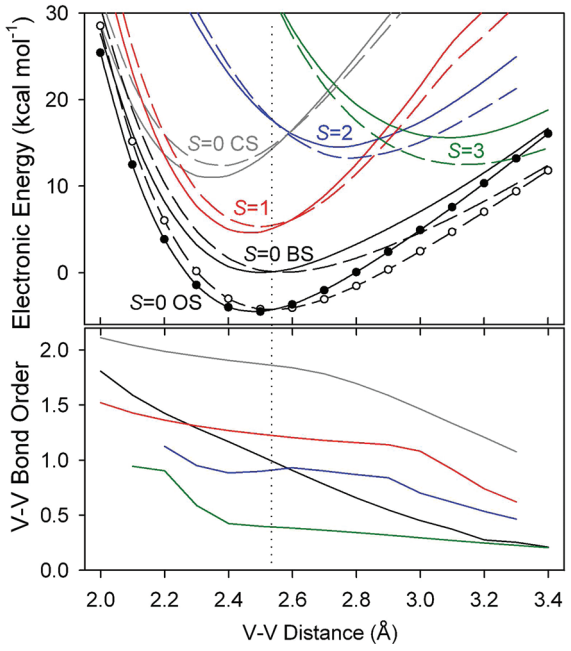

Figure 3. Potential energy surfaces and metal−metal bond order profiles calculated for the BS singlet (black lines), the OS singlet after the spin-projection correction has been applied (black lines with circles), CS singlet (gray), triplet (red), pentet (blue), and septet (green) electronic states of $[V(C_5H_5)]_2Pn$ at the PBE/TZVP and PBE-D/TZVP levels of theory (dashed and solid lines, respectively). All electronic energies are referenced to the energy of the BS singlet. A dotted vertical line indicates a value of the V−V distance from the X-ray structure.

OS singlet is the ground state in the 2.0−3.3 Å range of the V−V internuclear distance. At very long metal−metal distances, the OS singlet and the septet state become degenerate because of the loss of the metal−metal interaction. The PBE and PBE-D calculations predict the energy minimum near the experimental value of the V−V distance (2.54 Å). The V−V bond order for the ground electronic state decreases from ∼1.0 at the energy minimum to 0.25 at 3.3 Å (Figure 3). Furthermore, the close proximity with the triplet state with the energy of 4.5 kcal mol^{-1} (Figure 3, Table 1) accounts for the experimentally observed partial paramagnetism.[25] The lowest-energy S = 2 and S = 3 excited states exhibit the PES minima at longer V−V distances and show weaker covalent interactions between the two V atoms than the singlet ground state.

These observations confirm that in this π-ligand bridged dimer, the V−V interaction is consistently weak and corresponds to a single metal−metal bond at the energy minimum. The bonding within the complex is dominated by the vanadium−Pn ligand interactions (Figure 4). The Mayer bond order between the two $[V^{II}(C_5H_5)]^+$ (S = 3/2) fragments is only 1.40, while the bond order between each of the two $[V^{II}(C_5H_5)]^+$ fragments and the Pn^{2-} ligand is 2.34. Donation from the Pn^{2-} ligand to the $[V^{II}(C_5H_5)]^+$ fragment (2.76 electrons) is a major contributor to the metal−Pn ligand bonding. On the Pn^{2-} ligand side, five occupied π orbitals (see Figure S1 in the Supporting Information) contribute the most to the ligand-to-metal donation. The V-to-Pn ligand back-donation (0.67 electrons) is also significant.

The spin localization for the ground state of $[V(C_5H_5)]_2Pn$ is evident from values of V atomic spin densities (Table 1), the examination of the frontier orbitals (Figure 5), and the value of

dx.doi.org/10.1021/ct3000124 | J. Chem. Theory Comput. 2012, 8, 908−914

Table 1. Metal−Metal Distances, Mayer Bond Orders, Vanadium Atomic Spin Densities (SD) for the Broken-Symmetry Singlet Ground State, and the Electronic Energies of the Lowest Triplet and Closed-Shell Singlet States of $[V(C_5H_5)]_2Pn$

XC functional	XC class	d_{V-V} (Å)	B_{V-V}	SD_V[c] (au)	$\Delta E_{BS\text{-}Triplet}$[d] (kcal mol^{-1})	$\Delta E_{BS\text{-}CS}$[e] (kcal mol^{-1})
experiment[a]		2.538			4.1[f]	
PW91-PW91	GGA	2.565	0.95	2.00	5.3	12.2
B−P86	GGA	2.568	0.96	1.98	5.1 (4.0)[g]	12.0 (9.9)[g]
PBE-PBE	GGA	2.572	0.95	1.99	5.3 (4.6)[g]	12.3 (11.0)[g]
TPSS−TPSS	meta-GGA	2.575	0.87	2.11	6.1 (4.8)[g]	15.7 (13.2)[g]
VSXC	meta-GGA	2.585	0.82	2.36	12.0	17.3
B-LYP	GGA	2.614	0.96	2.06	5.9 (4.5)[g]	12.0 (9.5)[g]
G96-LYP	GGA	2.620	0.92	2.10	6.0	12.6
B97D	GGA	2.659	0.67	2.58	10.6	17.6
PKZB−PKZB	meta-GGA	2.660	0.76	2.35	7.5	16.9
M06L	GGA	2.681	0.65	2.58	11.4	24.2
TPSSh	hybrid	2.759	0.46	2.66	13.6	31.1
τ-HCTH	meta-GGA	2.857	0.43	2.89	15.4	24.9
τ-HCTHhyb	hydrid	2.865	0.37	2.79	19.3	37.2
wB97XD[b]	hybrid	2.883	0.28	2.81	24.5	58.8
M06	hybrid	2.896	0.32	2.86	24.9	45.8
B3−P86	hybrid	2.907	0.27	2.87	22.4	44.8
PBE0-PBE	hybrid	2.946	0.23	2.93	29.4	72.3
BMK	hybrid	2.972	0.23	2.78	29.2	73.3
B3-LYP	hybrid	2.994	0.25	2.87	25.3 (20.9)[g]	46.7 (41.7)[g]
X3-LYP	hybrid	2.999	0.24	2.88	27.2	49.4
O3-LYP	hybrid	3.009	0.26	2.93	21.6	39.6

[a]Data from ref 25. [b]The functional includes the empirical dispersion correction. [c]Mulliken derived atomic spin density for V atoms. [d]The electronic energy difference between the BS singlet and the lowest-energy triplet state. [e]The electronic energy difference between the BS singlet and the CS singlet. [f]The experimental value corresponds to $\Delta H_{Singlet-Triplet}$. Calculated $\Delta H_{BS\text{-}Triplet}$ is only 0.1 kcal mol^{-1} smaller than $\Delta E_{BS\text{-}Triplet}$. [g]The energies after applying the dispersion correction.[51]

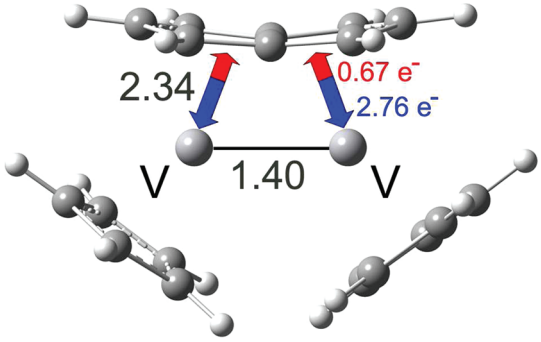

Figure 4. Mayer bond orders between the $[V^{II}(C_5H_5)]^+$ fragments and the Pn^{2-} ligand for the BS singlet of $[V(C_5H_5)]_2Pn$ at the PBE/TZVP level. Pn ligand-to-metal and metal-to-ligand charge donations are shown in blue and red, respectively.

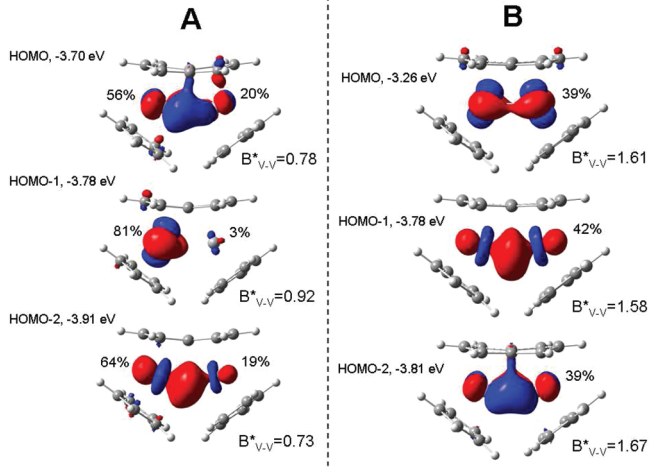

Figure 5. Three highest occupied molecular orbitals and occupancy-perturbed bond orders for the metal−metal interaction (B_{V-V}*) for the BS singlet (A) and CS singlet (B) states of $[V(C_5H_5)]_2Pn$ at the PBE/TZVP level. Orbital isosurface plots (at 0.05 au) also show the atomic contributions (%) from vanadium atoms.

the bond order for the V−V interaction (Figure 3 and Table 1). At the PBE/TZVP level of theory, the V−V bond order is 0.95 at the energy minimum. If an electron is removed from the HOMO, HOMO−1, or HOMO−2 of the complex, the V−V bond order decreases from 0.95 to 0.78, 0.92, or 0.73, respectively (Figure 5 and Table S1 in the Supporting Information). Such small decreases are indicative of small bonding contributions of these metal-based orbitals to the metal−metal interaction due to their localized character (Figure 5). On the other hand, the CS singlet has a stronger metal−metal bond (B_{V-V} = 1.92) with a shorter V−V distance (Figure 3), and its MOs are symmetric, with equal contributions from two V atoms (Figure 5).

Calculations of the lowest-energy singlet and triplet states of $[V(C_5H_5)]_2Pn$ using a wide range of popular XC functionals (GGA, meta-GGA, and hybrid) were performed, and the results are summarized in Table 1. GGA calculations reproduce the metal−metal distance, and $\Delta E_{BS\text{-}Triplet}$ matches the experimental singlet−triplet energy gap fairly well. The calculated V−V distances and bond orders range from 2.565 Å (PW91) to 2.681 Å (M06L) and from 0.65 (M06L) to 0.96 (BP86 and BLYP), respectively. $\Delta E_{BS\text{-}Triplet}$ values are typically in the 5.1−6.1 kcal mol^{-1} range. A further improvement of accuracy can be achieved by using the empirical dispersion corrections[51] that

dx.doi.org/10.1021/ct3000124 | J. Chem. Theory Comput. 2012, 8, 908−914

account for the fact that the non-Coulomb part of exchange functionals typically dies off too rapidly and becomes very inaccurate at large distances. After applying the long-range empirical dispersion corrections to the electronic energies from BP86, PBE, TPSS, and BLYP calculations, the corrected values of $\Delta E_{\text{BS-Triplet}}$ (4.0−4.8 kcal mol^{-1}) reproduce the experimental singlet−triplet energy gap very well. In addition to better energy predictions, the dispersion corrections also shift the position of PES minima toward shorter metal−metal distances (Figure 3). The BS singlet energy minimum shifts from a $d_{\text{V-V}}$ of 2.57 Å at the PBE level (Table 1) to a $d_{\text{V-V}}$ of 2.52 Å at the PBE-D level (Figure 3). The latter value is only slightly shorter than the experimental $d_{\text{V-V}}$ of 2.54 Å. The B97D and M06L functionals were the only GGA functionals for which $\Delta E_{\text{BS-Triplet}}$ exceeds the experimental singlet−triplet energy gap by more than 5 kcal mol^{-1}. M06L was also the GGA functional that gave a $d_{\text{V-V}}$ of 2.68 Å (Table 1), which is 0.14 Å longer than the X-ray value. GGA calculations without dispersion corrections place the CS singlet state 12−24 kcal mol^{-1} higher in energy relative to the BS singlet (Table 1). Dispersion corrections reduce this energy gap by 2−3 kcal mol^{-1}.

Application of Yamaguchi's approximate spin-projection method[68,69] to obtain the energy of the *pure* singlet state (Figure 3) leads to a lowering of the energy of the open-shell singlet state by 4.2 kcal mol^{-1} (PBE) and 4.5 kcal mol^{-1} (PBE-D) relative to the energy of the BS singlet. The energy minimum for the OS singlet exhibits almost no V−V distance shift relative to the corresponding BS singlet minimum from the PBE and PBE-D calculations.

Meta-GGA functionals tend to predict a longer $d_{\text{V-V}}$ and a bigger singlet−triplet energy gap ($\Delta E_{\text{BS-Triplet}}$ of 6.1−15.4 kcal mol^{-1}, Table 1). Overall, performance of these meta-GGA functionals (except τ-HCTH) is relatively close to the performance of the GGA functionals.

BS calculations using hybrid XC functionals, including a popular B3LYP functional, performed rather poorly for both structural and energy predictions for the $[V(C_5H_5)]_2Pn$ complex (Table 1 and Figure 6). The V−V distance (2.759−3.009 Å) is significantly longer (by at least 0.22 Å) than the X-ray distance. At such a large V−V distance, the Mayer bond order for the metal−metal interaction is quite small (0.23−0.46). The energy gap between the BS singlet and the triplet (13.6 to 29.4 kcal mol^{-1}) is 3 to 7 times greater than the experimental singlet−triplet energy gap, and the energy gap between the BS and CS singlets (31.1 to 73.3 kcal mol^{-1}) is also considerably greater than the corresponding gap from the GGA calculations (12.0 to 24.2 kcal mol^{-1}). Application of Yamaguchi's approximate spin-projection method[68,69] to obtain the energy of the *pure* singlet state (Figure 6) leads to further lowering of the energy of the open-shell singlet state by 3.0 kcal mol^{-1} relative to the energy of the BS singlet. However, the energy minimum for the OS singlet with the Yamaguchi spin-projection correction shows a shift for the V−V distance to ∼2.7 Å from 2.9 Å for the BS solution at the B3LYP-D/TZVP level of theory.

These results point to the fact that the current hybrid XC functionals are deficient in maintaining a balanced description of metal−metal and metal−ligand interactions for systems with weak-to-intermediate metal−metal interactions such as the $[V(C_5H_5)]_2Pn$ complex. These XC functionals overestimate the stability of the singlet states with the antiferromagnetically coupled HS metal ions relative to the lowest-energy triplet state and the singlet states with stronger metal−metal interactions

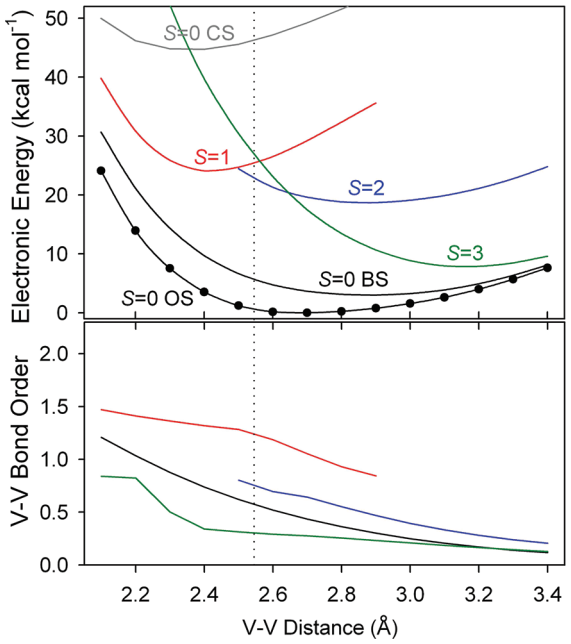

Figure 6. Potential energy surfaces and metal−metal bond order profiles calculated for the BS singlet (black line), the OS singlet after the spin-projection correction has been applied (black line with circles), CS singlet (gray), triplet (red), pentet (blue), and septet (green) electronic states of $[V(C_5H_5)]_2Pn$ at the B3LYP-D/TZVP level. All electronic energies are referenced to the energy of the OS singlet. A dotted vertical line indicates a value of the V−V distance from the X-ray structure.

(compare PES data in Figures 3 and 6). It is important to point out this deficiency since many DFT calculations for TM complexes with metal−metal interactions are performed using hybrid XC functionals.

Since this failure of hybrid XC functionals for dimeric complexes parallels the overstabilization of HS states of mononuclear TM complexes, it is very likely that these two deficiencies have a common origin. The poor performance of hybrid functionals for TM diatomic molecules has also been pointed out by Truhlar and co-workers.[74] Test calculations on eight M_2 molecules showed that the GGA functionals were more accurate for the atomization energies of pure TM systems than are their meta or hybrid analogues.

■ CONCLUSIONS

The electronic structure of the vanadium dimer complex $[V(C_5H_5)]_2Pn$ with a single metal−metal bond was characterized, and the energies of the relevant spin states were evaluated. To simplify evaluation of orbital contributions to bonding between atoms and fragments, orbital occupancy-perturbed bond orders were introduced. The geometry and experimentally determined singlet−triplet energy gap in this complex can be used to test the quality of modern XC functionals in order to determine their suitability for computational studies of complexes with metal−metal bonding. The majority of GGA functionals were determined to be quite suitable to reproduce the metal−metal distance and the single−triplet gap in $[V(C_5H_5)]_2Pn$. Further accuracy improvement can be achieved by using empirical dispersion corrections. On the other hand, hybrid XC functionals, including the widely used B3LYP functional, performed rather poorly for spin state energy predictions. In parallel to their overstabilization of HS

dx.doi.org/10.1021/ct3000124 | J. Chem. Theory Comput. 2012, 8, 908−914

states in mononuclear TM complexes, the hybrid XC functionals overestimate the stability of the OS singlet state with the antiferromagnetically coupled HS metal ions relative to the lowest-energy triplet state and the singlet state with stronger metal−metal bonds. Thus, these hybrid XC functionals are less suitable for computational studies of multinuclear 3d transition metal complexes with weak-to-intermediate metal−metal bonding.

■ ASSOCIATED CONTENT

Supporting Information

Optimized atomic coordinates for the ground state structures and the occupied fragment orbitals of the pentalene (Pn^{2-}) ligand that contribute to ligand-to-metal donation in the complex. This information is available free of charge via the Internet at http://pubs.acs.org.

■ AUTHOR INFORMATION

Corresponding Author

*E-mail: sgorelsk@uottawa.ca.

Notes

The authors declare no competing financial interest.

■ ACKNOWLEDGMENTS

We thank the Centre for Catalysis Research and Innovation (CCRI) and the University of Ottawa for supporting this work. We also thank Prof. Tom K. Woo (University of Ottawa) for use of the computing facilities funded by the Canada Foundation for Innovation and the Ontario Research Fund.

■ REFERENCES

(1) Cotton, F. A.; Murillo, L. A.; Walton, R. A. *Multiple Bonds Between Metal Atoms*, 3rd ed.; Springer: Berlin, 2005.
(2) Miskowski, V. M.; Hopkins, M. D.; Winkler, J. R.; Gray, H. B. In *Inorganic Electronic Structure and Spectroscopy*; Solomon, E. I., Lever, A. B. P., Eds.; Wiley-Interscience: New York, 1999; Vol. 2, pp 343−402.
(3) Berry, J. F. *Struct. Bonding (Berlin)* **2010**, *136*, 1−28.
(4) Ni, C.; Power, P. P. *Struct. Bonding (Berlin)* **2010**, *136*, 59−112.
(5) Nguyen, T.; Sutton, A. D.; Brynda, M.; Fettinger, J. C.; Long, G. J.; Power, P. P. *Science* **2005**, *310*, 844−847.
(6) Kreisel, K. A.; Yap, G. P. A; Dmitrenko, O.; Landis, C. R.; Theopold, K. H. *J. Am. Chem. Soc.* **2007**, *129*, 14162−14163.
(7) Wolf, R.; Ni, C.; Nguyen, T.; Brynda, M.; Long, G. J.; Sutton, A. D.; Fischer, R. C.; Fettinger, J. C.; Hellman, M.; Pu, L. H.; Power, P. P. *Inorg. Chem.* **2007**, *46*, 11277−11290.
(8) Hsu, C. W.; Yu, J. S. K.; Yen, C. H.; Lee, G. H.; Wang, Y.; Tsai, Y. C. *Angew. Chem., Int. Ed.* **2008**, *47*, 9933−9936.
(9) Horvath, S.; Gorelsky, S. I.; Gambarotta, S.; Korobkov, I. *Angew. Chem., Int. Ed.* **2008**, *47*, 9937−9940.
(10) Noor, A.; Wagner, F. R.; Kempe, R. *Angew. Chem., Int. Ed.* **2008**, *47*, 7246−7249.
(11) Noor, A.; Kempe, R. *Chem. Rec.* **2010**, *10*, 413−416.
(12) Noor, A.; Glatz, G.; Muller, R.; Kaupp, M.; Demeshko, S.; Kempe, R. *Nat. Chem.* **2009**, *1*, 322−325.
(13) Wagner, F. R.; Noor, A.; Kempe, R. *Nat. Chem.* **2009**, *1*, 529−536.
(14) Noor, A.; Glatz, G.; Muller, R.; Kaupp, M.; Demeshko, S.; Kempe, R. *Z. Anorg. Allg. Chem.* **2009**, *635*, 1149−1152.
(15) Brynda, M.; Gagliardi, L.; Widmark, P. O.; Power, P. P.; Roos, B. O. *Angew. Chem., Int. Ed.* **2006**, *45*, 3804−3807.
(16) Landis, C. R.; Weinhold, F. *J. Am. Chem. Soc.* **2006**, *128*, 7335−7345.
(17) Frenking, G.; Tonner, R. *Nature* **2007**, *446*, 276−277.
(18) La Macchia, G.; Aquilante, F.; Veryazov, V.; Roos, B. r. O.; Gagliardi, L. *Inorg. Chem.* **2008**, *47*, 11455−11457.
(19) Wu, L.-C.; Hsu, C.-W.; Chuang, Y.-C.; Lee, G.-H.; Tsai, Y.-C.; Wang, Y. *J. Phys. Chem. A* **2011**, *115*, 12602−12615.
(20) Hay, P. J.; Thibeault, J. C.; Hoffmann, R. *J. Am. Chem. Soc.* **1975**, *97*, 4884−4899.
(21) McGrady, J. E.; Stranger, R.; Lovell, T. *J. Phys. Chem. A* **1997**, *101*, 6265−6272.
(22) Gorelsky, S. I. Ab Initio and Semiempirical Methods. In *Computational Inorganic and Bioinorganic Chemistry*; Solomon, E. I., Scott, R. A., King, R. B., Eds.; John Wiley & Sons: Chichester, U.K., 2009; pp 43−54.
(23) De Mello, P. C.; Edwards, W. D.; Zerner, M. C. *Int. J. Quantum Chem.* **1983**, *23*, 425−436.
(24) Edema, J. J. H.; Gambarotta, S. *Comments Inorg. Chem.* **1991**, *4*, 195.
(25) Jones, C. J.; O'Hare, D. *Chem. Commun.* **2003**, 2208−2209.
(26) Bachmann, B.; Hahn, F.; Heck, J.; Wuensch, M. *Organometallics* **1989**, *8*, 2523−2543.
(27) Perdew, J. P.; Burke, K.; Ernzerhof, M. *Phys. Rev. Lett.* **1996**, *77*, 3865−3868.
(28) Schafer, A.; Huber, C.; Ahlrichs, R. *J. Chem. Phys.* **1994**, *100*, 5829−5835.
(29) Ilango, S.; Vidjayacoumar, B.; Gambarotta, S.; Gorelsky, S. I. *Inorg. Chem.* **2008**, *47*, 3265−3273.
(30) Noodleman, L. *J. Chem. Phys.* **1981**, *74*, 5737−5743.
(31) Noodleman, L.; Davidson, E. R. *Chem. Phys.* **1986**, *109*, 131−143.
(32) Cotton, F. A.; Chen, H.; Daniels, L. M.; Feng, X. *J. Am. Chem. Soc.* **1992**, *114*, 8980−8993.
(33) Petrie, S.; Stranger, R. *Inorg. Chem.* **2004**, *43*, 2597−2610.
(34) Reiher, M.; Salomon, O.; Hess, B. A. *Theor. Chem. Acc.* **2001**, *107*, 48−55.
(35) Fouqueau, A.; Casida, S. M. M. E.; Daku, L. M. L.; Hauser, A.; Neese, F. *J. Chem. Phys.* **2004**, *120*, 9473−9486.
(36) Fouqueau, A.; Casida, M. E.; Daku, L. M. L.; Hauser, A.; Neese, F. *J. Chem. Phys.* **2005**, *122*, 044110.
(37) Vancoillie, S.; Zhao, H.; Radon, M.; Pierloot, K. *J. Chem. Theory Comput.* **2010**, *6*, 576−582.
(38) Harvey, J. N. *Struct. Bonding (Berlin)* **2004**, *112*, 151−183.
(39) Timmer, G. H.; Berry, J. F. *C. R. Chim.* **2012**, *15*, 192−201.
(40) Ahlrichs, R.; Furche, F.; Grimme, S. *Chem. Phys. Lett.* **2000**, *325*, 317−321.
(41) Frisch, M. J.; Trucks, G. W.; Schlegel, H. B.; Scuseria, G. E.; Robb, M. A.; Cheeseman, J. R.; Scalmani, G.; Barone, V.; Mennucci, B.; Petersson, G. A.; Nakatsuji, H.; Caricato, M.; Li, X.; Hratchian, H. P.; Izmaylov, A. F.; Bloino, J.; Zheng, G.; Sonnenberg, J. L.; Hada, M.; Ehara, M.; Toyota, K.; Fukuda, R.; Hasegawa, J.; Ishida, M.; Nakajima, T.; Honda, Y.; Kitao, O.; Nakai, H.; Vreven, T.; Montgomery, J. A., Jr.; Peralta, J. E.; Ogliaro, F.; Bearpark, M.; Heyd, J. J.; Brothers, E.; Kudin, K. N.; Staroverov, V. N.; Kobayashi, R.; Normand, J.; Raghavachari, K.; Rendell, A.; Burant, J. C.; Iyengar, S. S.; Tomasi, J.; Cossi, M.; Rega, N.; Millam, N. J.; Klene, M.; Knox, J. E.; Cross, J. B.; Bakken, V.; Adamo, C.; Jaramillo, J.; Gomperts, R.; Stratmann, R. E.; Yazyev, O.; Austin, A. J.; Cammi, R.; Pomelli, C.; Ochterski, J. W.; Martin, R. L.; Morokuma, K.; Zakrzewski, V. G.; Voth, G. A.; Salvador, P.; Dannenberg, J. J.; Dapprich, S.; Daniels, A. D.; Farkas, Ö.; Foresman, J. B.; Ortiz, J. V.; Cioslowski, J.; Fox, D. J. *Gaussian 09*, revision A.02; Gaussian, Inc.: Wallingford, CT, 2009.
(42) Perdew, J. P.; Chevary, J. A.; Vosko, S. H.; Jackson, K. A.; Pederson, M. R.; Singh, D. J.; Fiolhais, C. *Phys. Rev. B* **1992**, *46*, 6671−6687.
(43) Perdew, J. P.; Wang, Y. *Phys. Rev. B* **1992**, *45*, 13244−13249.
(44) Perdew, J. P. *Phys. Rev. B* **1986**, *33*, 8822−8824.
(45) Becke, A. D. *Phys. Rev. A* **1988**, *38*, 3098−3100.
(46) Tao, J. M.; Perdew, J. P.; Staroverov, V. N.; Scuseria, G. E. *Phys. Rev. Lett.* **2003**, *91*, 146401.
(47) Van Voorhis, T.; Scuseria, G. E. *J. Chem. Phys.* **1998**, *109*, 400−410.
(48) Lee, C.; Yang, W.; Parr, R. G. *Phys. Rev.* **1988**, *B37*, 785−789.
(49) Gill, P. M. W. *Mol. Phys.* **1996**, *89*, 433−445.

(50) Adamo, C.; Barone, V. *J. Comput. Chem.* **1998**, *19*, 418−429.
(51) Grimme, S. *J. Comput. Chem.* **2006**, *27*, 1787−1799.
(52) Perdew, J. P.; Kurth, S.; Zupan, A.; Blaha, P. *Phys. Rev. Lett.* **1999**, *82*, 2544−2547.
(53) Zhao, Y.; Truhlar, D. G. *J. Chem. Phys.* **2006**, *125*, 194101.
(54) Boese, A. D.; Handy, N. C. *J. Chem. Phys.* **2002**, *116*, 9559−9569.
(55) Chai, J.-D.; Head-Gordon, M. *Phys. Chem. Chem. Phys.* **2008**, *10*, 6615−6620.
(56) Zhao, Y.; Truhlar, D. G. *Theor. Chem. Acc.* **2008**, *120*, 215−241.
(57) Becke, A. D. *J. Chem. Phys.* **1993**, *98*, 5648−5652.
(58) Perdew, J. P.; Ernzerhof, M.; Burke, K. *J. Chem. Phys.* **1996**, *105*, 9982−9985.
(59) Adamo, C.; Barone, V. *J. Chem. Phys.* **1999**, *110*, 6158−6170.
(60) Boese, A. D.; Martin, J. M. L. *J. Chem. Phys.* **2004**, *121*, 3405−3416.
(61) Cohen, A. J.; Handy, N. C. *Mol. Phys.* **2001**, *99*, 607−615.
(62) Seeger, R.; Pople, J. A. *J. Chem. Phys.* **1977**, *66*, 3045−3050.
(63) Gorelsky, S. I.; Lever, A. B. P. *J. Organomet. Chem.* **2001**, *635*, 187−196.
(64) Gorelsky, S. I.; Basumallick, L.; Vura-Weis, J.; Sarangi, R.; Hodgson, K. O.; Hedman, B.; Fujisawa, K.; Solomon, E. I. *Inorg. Chem.* **2005**, *44*, 4947−4960.
(65) Gorelsky, S. I.; Solomon, E. I. *Theor. Chem. Acc.* **2008**, *119*, 57−67.
(66) Gorelsky, S. I. *AOMix: Program for Molecular Orbital Analysis*, version 6.56; University of Ottawa: Ottawa, Canada, 2012.
(67) Cohen, A. J.; Mori-Sánchez, P.; Yang, W. *Science* **2008**, *321*, 792−794.
(68) Yamaguchi, K.; Jensen, F.; Dorigo, A.; Houk, K. N. *Chem. Phys. Lett.* **1988**, *149*, 537−542.
(69) Yamaguchi, K.; Okumura, M.; Mori, W.; Maki, J.; Takada, K.; Noro, T.; Tanaka, K. *Chem. Phys. Lett.* **1993**, *210*, 201−210.
(70) Mayer, I. *Int. J. Quantum Chem.* **1986**, *29*, 477−483.
(71) Gorelsky, S. I.; Ghosh, S.; Solomon, E. I. *J. Am. Chem. Soc.* **2006**, *128*, 278−290.
(72) Solomon, E. I.; Gorelsky, S. I.; Dey, A. *J. Comput. Chem.* **2006**, *27*, 1415−1428.
(73) Rusanova, J.; Rusanov, E.; Gorelsky, S. I.; Christendat, D.; Popescu, R.; Farah, A. A.; Beaulac, R.; Reber, C.; Lever, A. B. P. *Inorg. Chem.* **2006**, *45*, 6246−6262.
(74) Schultz, N. E.; Zhao, Y.; Truhlar, D. G. *J. Phys. Chem. A* **2005**, *109*, 4388−4403.